ASIAN JOURNAL OF CIVIL ENGINEERING (BUILDING AND HOUSING) VOL. 4, NOS 2-4 (2003)
PAGES 135-148

CYCLIC STRENGTH AND DUCTILITY OF RUSTED STEEL MEMBERS

S. M. Zahrai*
Department of Civil Engineering,
University of Tehran, Tehran, Iran, and
Department of Structural Engineering, Building and Housing Research Center, Tehran, Iran

ABSTRACT

After some recent earthquakes that demonstrated the potential seismic vulnerability of some types of steel bridges, many transportation agencies have initiated programs to evaluate the seismic resistance of their existing bridges. However in some regions, the problem will be more severe by the fact that steel bridges have frequently been exposed, for years, to an aggressive corrosive environment, particularly where road de-icing salts have been heavily used, seismic-resistant members frequently appear to be severely corroded. Similar problems occur to other steel structures. To determine whether such rusted members can reliably exhibit stable ductile behavior that is expected during an earthquake, a number of rusted pieces (having up to a 60% loss of cross-sectional area) taken from an old steel bridge, were subjected to some tension and cyclic bending tests.

Non-cyclic tension stress-capacity and ductility did not change significantly due to corrosion. However, cyclic tests showed that, while stable hysteretic behavior comparable to that of unrusted specimen is possible, premature low-cycle fatigue, typically develops. Irregularities along the rusted surface apparently act as crack initiators and precipitate crack propagation throughout the section

Keywords: corrosion, steel bridges, seismic resistance, cyclic bending, ductility, low-cycle fatigue, hysteretic energy

1. INTRODUCTION

Corrosion is the major cause of deterioration of steel structures. The results of this deterioration generally range from progressive weakening of a steel structure over a long time ,to rapid structural failure. Significant developments have appears for a better understanding of the causes of corrosion, enhance the corrosion-resistance of new steel structures, and provide structural evaluation methods to assess the safe strength of existing corroded structures. Indeed, many codes now specifically require corrosion protection in steel structures, specially those structures located in severe environments. Such protection is provided by means of suitable

* E-mail address of the corresponding author: mzahrai@ut.ac.ir

alloying elements in the steel, protective coatings, provision of extra thickness as a corrosion allowance, or other approved means. The type and degree of corrosion protection to be provided should be indicated on the structural drawings [4].

The corrosion of steel is a chemical change of iron to iron oxide consequently to current flow. In other words, it is an electrochemical process similar to the situation that occurs in a battery, where oxygen and an electrolyte are needed. For the corrosion conditions mostly observed in bridge members for instance, the electrolyte is a solution of salts or other chemical compounds in water. Ions, electrically charged particles formed by the division of salts in water, cannot carry current under dry conditions, so the presence of water is crucial for the corrosion process to occur. An aggressive environment and inadequate maintenance generally cause this corrosion. Figure 1 schematically illustrates the corrosion process. The consequence of corrosion is a reduction in member cross-sectional area and, in turn, strength; a reduction in the carrying capacity and structural safety.

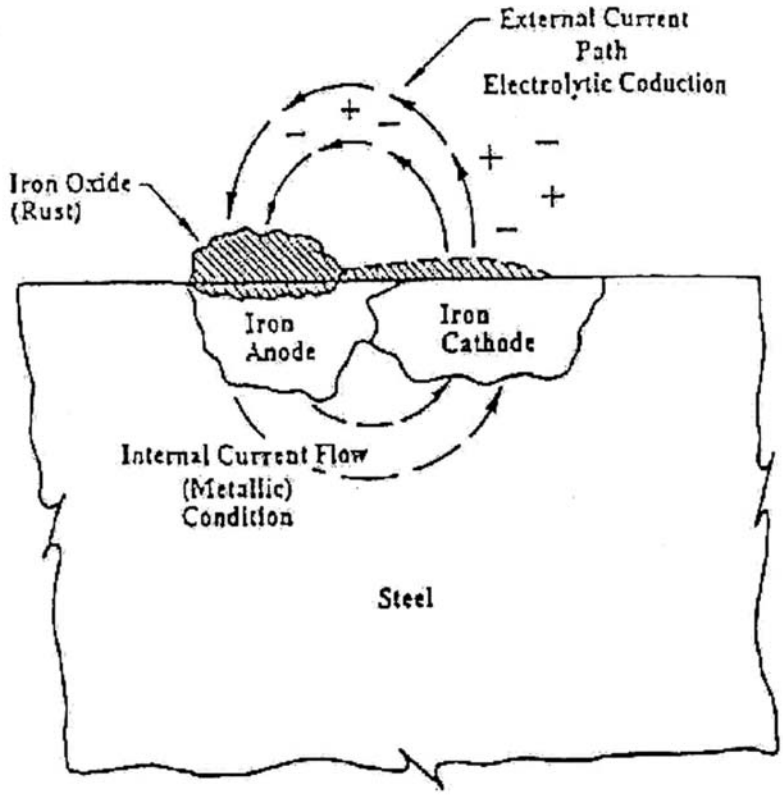

Figure 1. Schematic illustration of the corrosion process

The corrosion pattern that most commonly develop in steel bridges is the corrosion of the webs at the ends of the girder, and the corrosion of the bottom portion of the girder, along the entire length. Figures 2a and 2b show examples of different kinds of corrosion penetration in a few components and connections of a steel bridge.

Previous researchers have identified at least six forms of corrosion that influence the performance of structural steels used for the construction of bridges: uniform corrosion, galvanic

corrosion, crevice corrosion, pitting corrosion, stress corrosion, and corrosion fatigue [1,4]. Among these, uniform corrosion, with metal oxidation taking place uniformly over the entire exposed surface, is the most common and accounts for the greatest destruction of metal on a tonnage basis. Simple theories also exist to describe the mechanisms of uniform corrosion and the rate of expected corrosion in various environments. However, no theory could be found in the existing structural engineering literature commenting on the impact of corrosion on the fundamental cyclic ductility of structural steel.

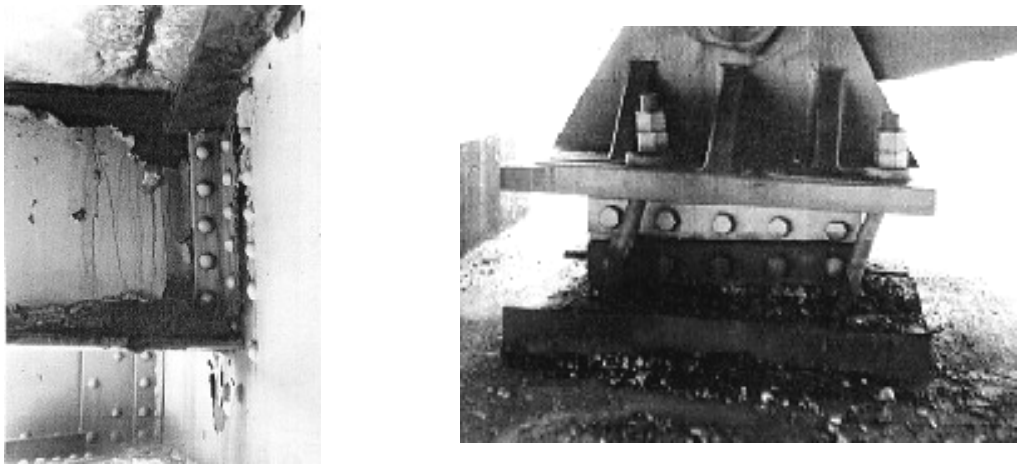

(a) (b)

Figure 2. (a) Typical areas of section loss to the flanges and web of stringers; (b) Typical condition of expansion bearings with many bolts bent or sheared off [1]

Recent earthquakes worldwide have shown that steel bridges can be vulnerable. Further to these earthquakes, numerous transportation agencies have started programs to evaluate the seismic vulnerability of their existing bridge inventory. However, in many parts of North America, the problem is complicated by the fact that steel bridges have frequently been exposed for years to an aggressive corrosion environment, particularly where road de-icing salts have been heavily used. As a result, many of the key structural members located along the critical seismic-resistance load paths are severely corroded. Much knowledge exists on the nature of corrosion and how to enhance the corrosion-resistance of new steel bridges, but there is no published information on the seismic performance of corroded members. To investigate this problem, a number of components were taken from a rusted steel bridge and subjected to tension tests and cyclic bending tests to various level of ductility intensities. Specimens had up to 60% cross-sectional loss due to corrosion. Similarly, some simple riveted connections, uniformly rusted, were also tested, in shear and in tension. This paper reports the results of this experimental work in terms of strength, ductility, cyclic ductility, and cumulative hysteretic energy, in the perspective of seismic resistance.

It is noteworthy that a limited number of fatigue-related experiments [1, 2, 3] indicate that, as a results of stress concentrations introduced by rust and rust-related notches, corroded base metal and details in steel bridge components could have a lower fatigue life than unrusted steel of

equivalent remaining cross-sectional area. However, no significant reduction of the monotonic structural ductility of tested specimens was reported [3].

2. NON-CYCLIC MATERIAL DUCTILITY

Although the available literature suggests that a ductile non-cyclic behavior is somewhat expected, the material under consideration here was first tested under monotonically increasing static load to establish its non-cyclic ductility, for better comparison with the cyclic tests results presented in a subsequent section. The rusted steel specimens available for this study were obtained from a bridge constructed in Ontario in the 1950s (demolished and replaced in 1991). The original structural drawings called for medium steel, likely a CAN/CSA G40.4 structural steel (equivalent to ASTM-A7 steel), had a nominal yield stress of 33 ksi (230 MPa).

To obtain the complete stress-strain relationship for the existing rusted steel material, coupons were extracted from a severely rusted floorbeam; two were taken from the web and one from the flange, all three flame-cut in the longitudinal direction of the floorbeam. Then, they were machined in accordance with the ASTM E8M specification with an 8 inch (200 mm) gage length with the important exception that the wide sides of the steel coupons were left unmachined to preserve their rusted surfaces. Maximum loss of cross-sectional area due to corrosion, as given by the least average thickness measured across an interval, are 61.5%, 36.2%, and 6.3% for the Flange (original thickness of 18.5 mm), Web 1 and Web 2 (original thickness of 11.6 mm) coupon specimens, respectively.

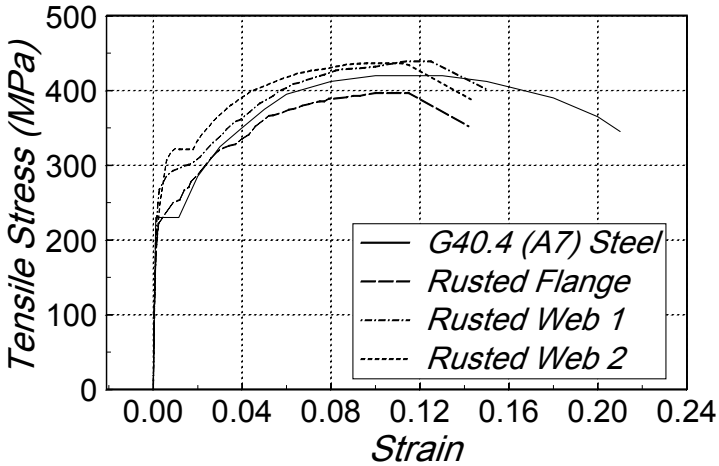

Figure 3. Experimentally obtained stress-strain curves for rusted coupons compared with that of unrusted A7 steel

Test results in terms of stress versus strain are presented in Figure 3, where the expected loss of strength is directly proportional to the loss in cross-sectional area. Stresses were obtained by dividing the applied load by the cross-sectional area at the minimum average thickness along the gage length. Expected result for comparable unrusted G40.4 steel specimen is also plotted in this Figure, assuming minimum yield strength (F_y) of 33 ksi (230 MPa), tensile strength (F_u) of

60 ksi (420 MPa), and elongation in 8 in. (200 mm) of 21%. All coupons failed at their section of least measured cross-sectional area. As shown in Figure 3, although the yield stress threshold is not affected by the presence of corrosion, a well defined yield plateau does not exist for the severely corroded specimens. This is logical since the cross-sectional area varies continuously along the length of the specimen due to randomness in the corrosion attack. Also shown in that Figure, maximum elongations at failure, ε_{max}, of 14.2%, 15% and 16% were obtained for the rusted coupons. This is somewhat less than the specified elongation for G40.4 (A7) steel, but this loss of ductility can be mostly attributed to slightly premature necking initiation and a shorter descending branch of the stress-strain curve past that point. Considering that maximum strengths have been reached nearly at the same strain, the available non-cyclic material ductility can be deemed unaffected by corrosion, within the range of practical interest. Finally, although the obtained ultimate stress capacity of the flange coupon is below that of the web coupons and that of the specified strength for G40.4 (A7) steel, the difference remains within statistical expectations, recognizing that the mean yield stress across the flanges of rolled shapes is usually lower than the corresponding value in their web.

3. CYCLIC BENDING TESTS

3.1 Weak-axis bending of steel plates

Two severely rusted lacing steel plates, taken from a built-up member of the bridge, were subjected to cyclic flexure in a 3-point bending apparatus with a span of 360 mm. For each plate, originally 76 mm wide and 10.5 mm thick, thickness was measured at 15 locations around the point of maximum moment. For the first specimen, in a first phase of testing, very accurate measurements of load versus center span deflections were taken to record the cyclic hysteretic behavior of the corroded specimens. Figure 4a presents the results for the first five inelastic cycles. Onset of yielding was observed at an applied load of 2.15 kN, corresponding to a midspan deflection of 5.8 mm.

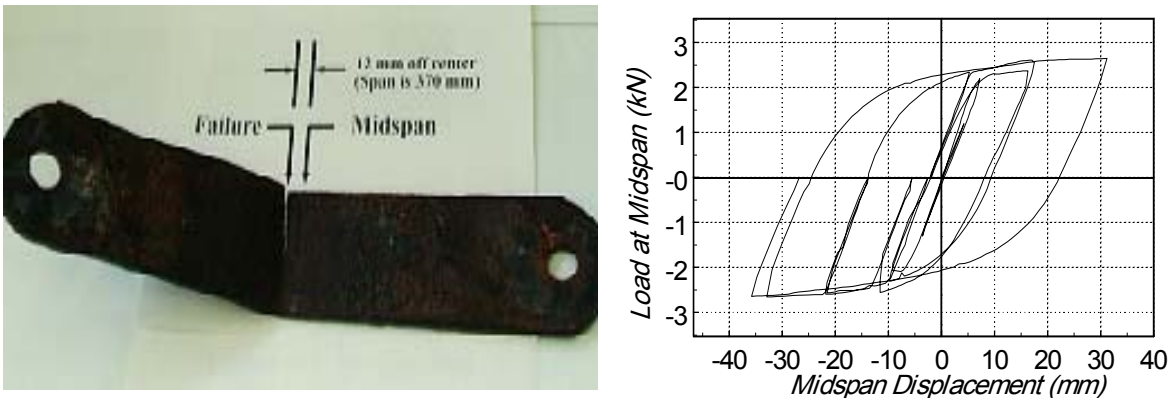

(a) (b)

Figure 4. (a) Cyclic load-displacement curves for plate specimen 1; (b) global view of this specimen after testing

Using the average measured thickness at the location of maximum moment (i.e. midspan), and steel strength, F_y , of 230 MPa, expected yield and plastic moments capacities were 0.131 kN-m and 0.196 kN-m respectively, corresponding to applied midspan loads of 1.46 kN and 2.18 kN. As minimum average thickness and remaining area are synonymous, this assessment of yield strength follows the procedure recommended by [1]. Likewise, midspan deflection at first yield was expected to be 3.7 mm. Given a good agreement between the experimentally obtained elastic stiffness (0.37 kN/mm) and theoretical one ($48EI/L^3$=0.39 kN/mm), the differences observed between experimental and analytical yield strengths and deflections can be partly attributable to the difficulty in accurately identifying experimentally the yield point for a specimen having an irregular cross-section, as well as to probable slightly greater than specified yield strength of the plates tested. It is noteworthy that loss of strength due to corrosion is considerable here as yield strength of the non-corroded lacing plate would have been 3.5 kN.

Then, to investigate the stability of these hysteretic loops under severe cyclic loading, it was decided to arbitrarily subject the specimen to 50 cycles at a maximum center deflection of 60 mm. For that specimen, this corresponded to a displacement ductility of 10.3 (i.e. 60/5.8). This number of cycles was somewhat arbitrarily selected, based on the argument that a stiff structure having a fundamental vibration period of 0.1 seconds and subjected to a severe earthquake having at least 25 seconds of strong motion would undergo at least 250 cycles of vibration, and quite possibly enter the inelastic range in 20% of those cycles. Survival to that severe test regime would have provided confidence in the cyclic ductile capacity of rusted steel members. In each of those large ductility cycles, a normalized hysteretic energy, $E_H/R_y\delta_y$, of 36 per cycle was dissipated until the 28th cycle when a “popping” noise was heard, when a 5 mm long crack oriented in the width direction was visible on the tension side of the member, approximately 1 mm wide and 1 mm deep. A normalized cumulative hysteretic energy of 1006 had been dissipated at that point. Testing resumed and an immediate drop in capacity was observed. Upon further cycling, the crack propagated in both directions, traveling towards the edges of the member as strength degradation worsened, Figure 5a, As seen in Figure 7a, after the 32th cycle, strength has fallen by 75%; the crack had spread through thickness and nearly across the entire width of the specimen, and testing was stopped, Figure 4b. Close-up view of other cracks of finite length parallel to the failure surface is shown in Figure 6. A second nearly identical specimen was similarly tested and nearly identical results were obtained, Figure 5b, Ref. [4].

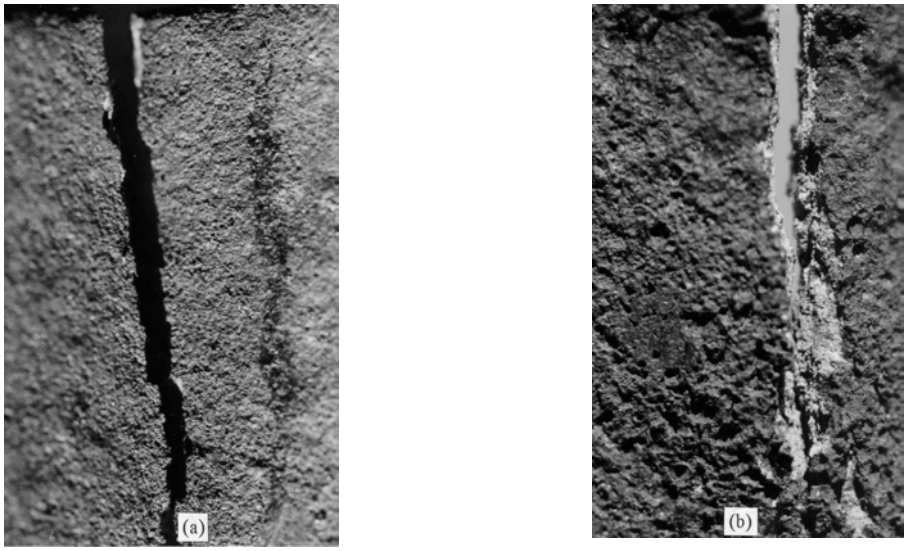

Figure 5. Close-up view of surface texture for three-point bending test specimens: (a) first cracking side of specimen 1; (b) last ruptured side of specimen 2

Figure 6. Close-up view of other cracks of finite length parallel to the failure surface

Information on the low-cycle fatigue of structural steel [5] indicates at least a 10-fold drop in low-cycle fatigue resistance for the maximum curvature ductility developed during this test. However, to provide an approximate experimental comparison benchmark, a 6.4 mm thick new plate of mild steel (of 300 MPa yield strength) was also tested. This new steel plate was subjected to 50 inelastic cycles at a center displacement of 60 mm, corresponding to a displacement ductility of 9, curvature ductility of 20, and normalized cumulative hysteretic energy of 1640 for 50 cycles without any sign of cracking or strength reduction, Figure 7b.

Conceptually, the above observed premature cracking under alternating plasticity can

be attributed to the presence of irregularities along the rusted surface that act as crack initiators and precipitate crack propagation throughout the section. Consequently, members with large corrosion notches or more severe level and types of corrosion than considered here would likely have an even lower cracking resistance under alternating plasticity, and their contribution to seismic resistance might be of even greater concern.

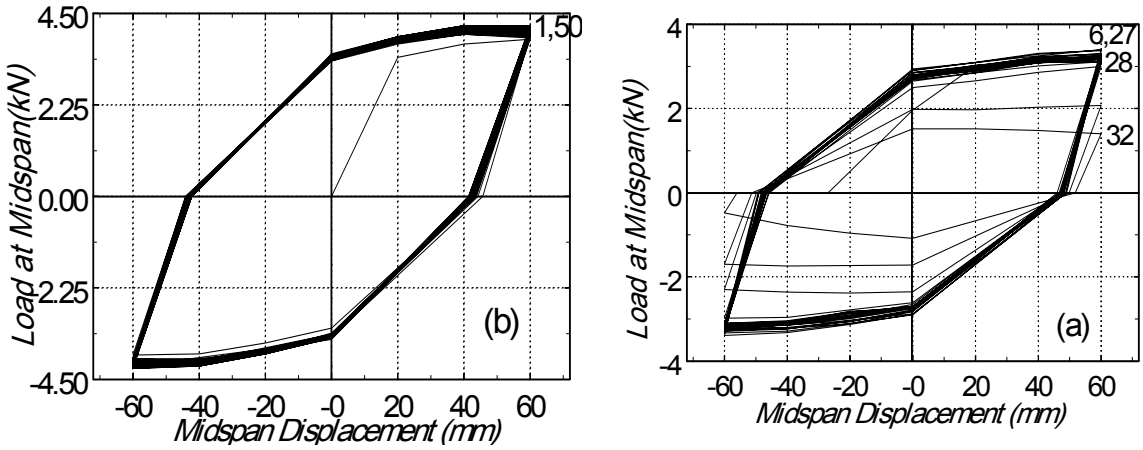

(a) rusted specimen for cycles 6 to failure; (b) unrusted specimen for all cycles

Figure 7. Simplified hysteretic behavior of plate specimens

3.2 Out-of-plane bending of web of structural s-shape

Additional tests were conducted to determine whether similar low-cycle fatigue failures would occur at lesser ductilities. The severely rusted web of a 350 mm-long floorbeam segment flame-cut from the same bridge was used for this next phase of testing. A simple set-up as shown in Figure 8, made it possible to subject the rusted web plate of this structural member to cyclic out-of-plane flexure. The flange of the section was bolted down to a rigid steel base itself anchored to a strong floor. Bolts were placed closely to eliminate rotation due to flexure of the flange. An horizontally placed servo-controlled actuator connected at mid-height of the web was used to cycle the cantilevering web in flexure about its weak axis, henceforth testing the most severely rusted portion of the web which happened to be near the web-flange intersection. The ends of the floorbeam segment were grinded to smoothen the flame-cut surfaces and eliminate any jagged edge, notch, or other stress raisers that could trigger crack initiation unrelated to the presence of corrosion. Prior to testing, thickness of the web in the critical areas (i.e. near the flanges) was measured with a micrometer and was found to vary between 6.7 and 12 mm, with average thicknesses of 9.8 mm at the critical section of specimen (original web thickness of 12.3 mm).

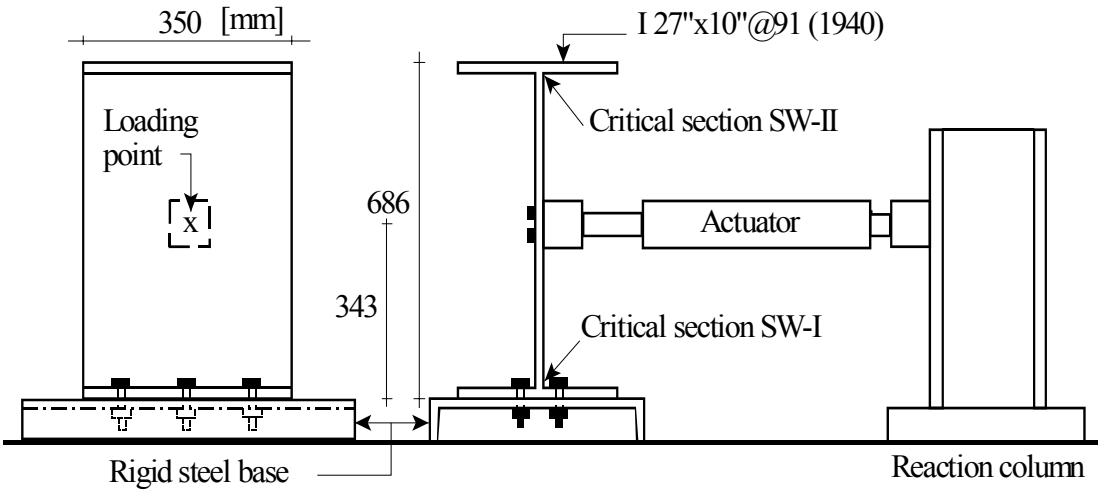

Figure 8. Test set-up for weak-axis bending of floor beam's rusted web

A high-resolution data acquisition system was used to record all data during the cyclic hysteretic testing of the corroded specimen. Since analytical estimates of the yield displacement proved difficult to accurately calculate, each test started by first subjecting the specimen to a few cycles of loading in search of the yield displacement.

For the first test, yield displacement was judged to occur at 12.5 mm based on first visible evidence of hysteretic behavior. The hysteretic displacement history was then programmed to apply 3 cycles at each of displacements of $\pm 0.5\delta_y$, $\pm 1.0\delta_y$, $\pm 2.0\delta_y$, $\pm 3.0\delta_y$, followed by 40 cycles at $\pm 4.0\delta_y$, 20 cycles at $\pm 6.0\delta_y$, and cycling to failure at $\pm 8.0\delta_y$. This follows the spirit of the ATC-24 testing protocol, albeit with more cycles at the range of inelastic deformations where low-cycle fatigue resistance data is sought. Loading rate was 1.0 cycle/minute.

The resulting load-displacement hysteretic curves for the first test are shown in Figure. 9a. During testing, a drop in the applied load necessary to push the specimen to displacements of $\pm 4.0\delta_y$ was noticed during the 40th load cycle (counting from the beginning of testing). This prompted closer examination of the specimen and discovery that a small hairline crack had appeared on both faces of the web, at roughly 50 mm from the south edge of the specimen and 60 mm above the base of the specimen. Five cycles later, the visible horizontal crack had grown to a length of 12.7 and 11.4 mm on the east and west web faces respectively. Strength degradation of 20% was observed after the 46th cycle (i.e. after 34 cycles at $4.0\delta_y$). By the 51st cycle, crack length had reached 26.6 and 14.5 mm on the east and west faces respectively, and strength had dropped nearly 40%, Figure 9b. Upon completion of the first cycle at $\pm 6.0\delta_y$, the crack had grown to a visible length of 270 and 184 mm on the east and west faces, tearing the specimen up to its south edge. Testing was stopped after the 56th cycle, at a displacement of $6.0\delta_y$, with only a 65 mm length of uncracked steel at the web's north edge, and a 80% strength degradation.

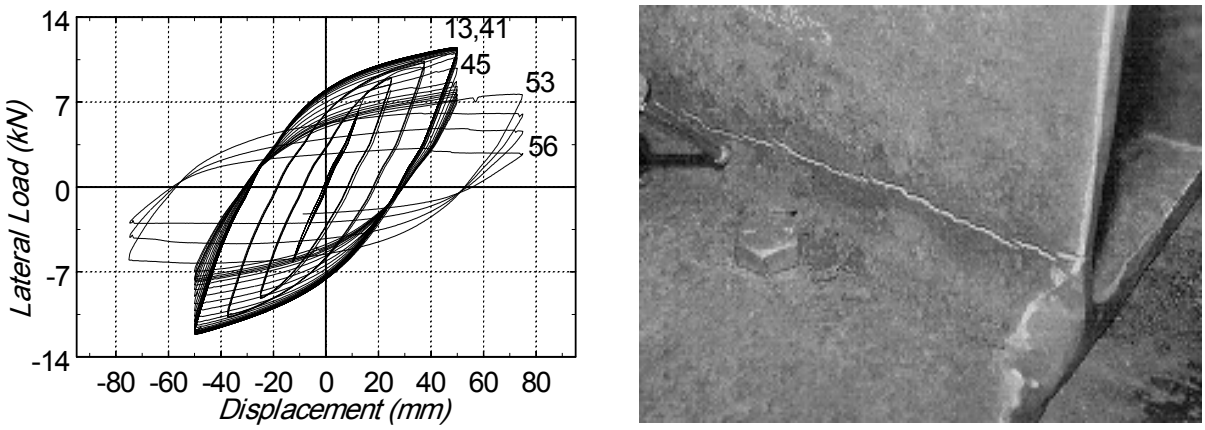

(a) (b)

Figure 9. (a) Hysteretic load-displacement curves for floor beam web specimen 1; (b) crack propagation in the specimen's web

Similar results were obtained by a second test [4]. It is notable that the definitions of yield strength and displacement have a considerable impact on all normalized quantities presented in this study. Since the 0.2% rule was found to be impracticable here, yield was generously defined as the onset of nonlinear behavior. If, in hindsight, yield point was defined by the intersection of the asymptotes to the experimentally obtained initial stiffness and stiffness at maximum resistance, yield displacements would typically become approximately 20 mm, making all calculated ductilities considerably smaller (with failures occurring at the same number of cycles, but typically at $2.5\delta_y$ rather than at $4.0\delta_y$, with considerably more alarming consequences).

4. ANALYTICAL PREDICTIONS OF MONOTONIC LOAD-DISPLACEMENT CURVE

An attempt was made to model the force-deformation curve of the rusted coupon specimen subjected to monotonic loading, relying solely on the availability of a limited number of thickness measurements taken with a micrometer and the theoretical stress-strain curve for the specified steel. The model considered treats the tension member as a piece-wise sequence of elements each having a cross-section equal to that measured across specimen width using linear thickness variation between the cross-width readings. For this purpose, the flange coupon was selected, and subdivided into 8 such segments of 25 mm length (considering the segments along the gage length).

Following this segmental procedure, as the load on the specimen is progressively increased, the corresponding stress, strain, and elongation is calculated for each segment (using the theoretical stress-strain relationship), and total elongation is obtained by adding the individual segment elongations.

To explore sensitivity of the results to the assumed length of the yield plateau, these

calculations were repeated three times, with yield plateau respectively ending at strains of 10, 15 or 20ε_y for each segment considered (true length of yield plateau length for A7 steel is approximately 12ε_y). Results, shown in Figure 10, in terms of force versus total elongation, compare well up to an elongation of 4 mm, corresponding to a strain elongation of 2%. This adequately covers the strain range of engineering significance for seismic-related problems. Beyond that, the model gives a more rapid strength rise, a lower failure elongation, and thus a far worse match against the experimental results. These differences can be attributed to unavoidable errors in obtaining a precise map of coupon thickness along the entire gage length and width, particularly due to limitations in the number of measurements taken, variations and irregularities in the rusted surface texture, and limited accuracy of the data collected using a micrometer with a head of 6 mm diameter on a surface with small asperities. Failing the availability of an accurate continuous measurement technique, it is difficult to improve this model. As for the model's lower elongation past the point of maximum strength, it is simply a consequence of assuming that necking develops in the critical segment having the minimum average thickness without further strain increases in the other segments. A more sophisticated model accounting for true strain (as opposed to engineering strain) and multi-dimensional plasticity interaction could lead to further improvements.

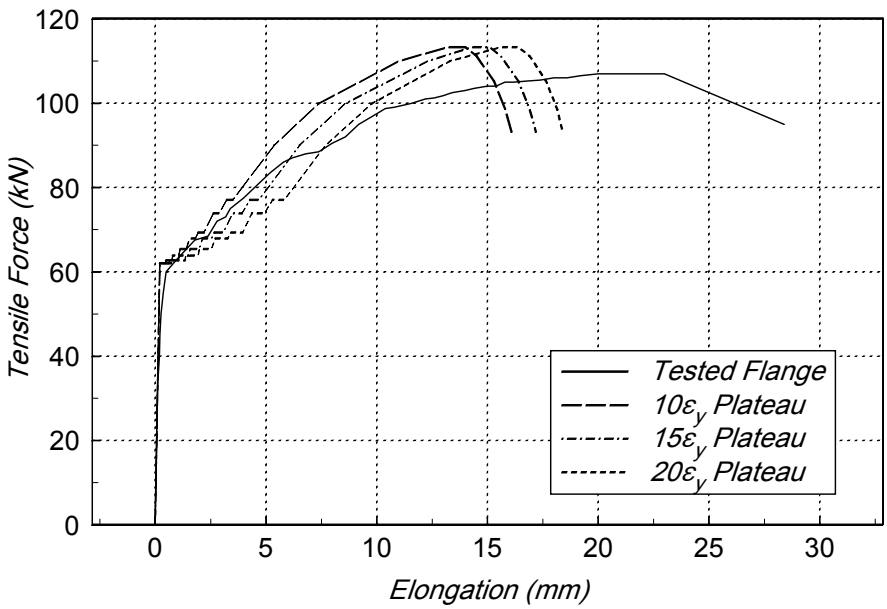

Figure 10. Analytically predicted monotonic load-displacement curves for different lengths of the yield plateau, compared to the corresponding curve for the tested flange coupon

Given the above difficulties in replicating the behavior of a specimen as simple as the tension coupon, further refinements to the model were not attempted. However, it is noteworthy that, in this case, the simple model used confirmed that all segments could yield prior to attainment of the ultimate strength along a given segment, because the ratio of maximum to minimum segment areas over the gage length of the coupon (A_{max}/A_{min}=335/270 = 1.24) was lower than the ratio of tensile to yield strength for this specimen (F_u/F_y = 1.83).

5. RIVET TESTS

Some riveted pieces were extracted from a few available rusted components to experimentally investigate the impact of corrosion on the tension and shear properties of rivets. By visual assessment of lost head area, rivets judged having most suffered from corrosion were selected among those available.

For the tension test, a rivet and its connected plates were isolated and cut out. Two segments were welded on sides of the specimen. With pulling on the segments, in turn pulling on the rivet, a tensile strength of 159 kN was obtained for this rivet, corresponding to an ultimate stress of 475 MPa when considering the rivet filled the entire 20.6 mm diameter hole when hot driven. Failure occurred by necking at the middle of the rivet's shank. This, as well as the experimentally obtained force-elongation curve, indicates no strength loss for rusted rivet.

A similar piece of rivet and connected pieces were isolated and cut out for a double-shear test. A special set-up was also built to create pure shear test conditions and insertion into an uniaxial testing machine, Figure 11a. An experimentally obtained ultimate shear strength of 240 kN (in double shear, or 120kN in single shear) was obtained for the rivet, with a corresponding shear deformation of 8 mm at failure as shown in Figure 11b. This is comparable to results reported in Ref. [6] for unrusted rivets.

(a) (b) (c)

Figure 11. (a) Special set-up to create pure shear test condition; (b) deformed shape of rivet at rupture; (c) close-up view of rupture surface showing minor rust on shank of rivet

Closer inspection of the failed rivets and surfaces revealed that corrosion had not progressed to significantly attack the shank of the rivets as shown in Figure 11c, in spite of the severe rust visible on the rivet heads. That condition can be attributed to the fact that hot rivets expand to fill their holes when driven during construction, and produce a clamping action as they cool and shrink after their installation. These mechanisms help confine the extent of severe corrosion to the rivet heads, and thus effectively prevent degradation of strength and ductility for rivets in

similar condition to those considered here, at least as long as a sufficient amount of rivet head remains to allow development of the rivet's tension resistance under that type of loading.

6. CONCLUSIONS

A limited test program was conducted to investigate the effect of uniform corrosion on the strength and ductility of members and connectors having uniform corrosion. The few available rivets tested in tension or shear did not exhibit any significant degradation of strength nor ductility, in spite of being judged severely rusted upon visual inspection. As for material taken from structural members, the non-cyclic tension yield and ultimate *stress* capacities, as well as the ductility of corroded members were apparently not significantly affected by the presence of rust, in spite of severe area loss. Use of minimum average thickness was reasonably effective in predicting yield and ultimate resistance.

Cyclic tests on structural members revealed that stable hysteretic behavior comparable to that of unrusted specimen is possible, but that premature fracture under alternating plasticity (i.e. low-cycle fatigue) will typically develop. Although a considerable cumulative hysteretic energy can be dissipated prior to the development of fatal cracking, it may not be sufficient to provide adequate seismic resistance. This low-cycle fatigue can be conceptually explained by the presence of irregularities along the rusted surface which may act as crack initiators and precipitate crack propagation throughout the section.

The simple model attempted to model the force-deformation curve of the rusted coupon specimen subjected to monotonic loading, confirmed that all segments could yield prior to attainment of the ultimate strength along a given segment of the specimen. Finally, close inspection of tested rivets and surfaces revealed that corrosion had not progressed to significantly attack the shank of the rivets.

Acknowledgements: The author would like to appreciate the financial support of the Natural Science and Engineering Research Council of Canada. He is also grateful to the technicians of the Structural Laboratory, Department of Civil Engineering, University of Canada, for their contribution in this research work.

REFERENCES

1. Kulicki, J. M., Prucz, Z., Sorgenfrei, D. F., Mertz, D. R. and Young, W. T., "Guidelines for evaluating corrosion effects in existing steel bridges.", *NCHRP Report 333*, Transportation Research Board, National Research Council, Washington, D.C., 1990.
2. Fisher, J. W., Yen, B. T. and Wang, D., "Fatigue strength of riveted bridge members.", *Journal of Structural Engineering*, *ASCE*, No. 11, **116**(1990) 2968-2981.
3. Fisher, J. W., Yen, B. T. and Wang, D., "Corrosion and its influence on strength of steel bridge members", Paper presented at 3rd Bridge Engrg. Conference, Denver, Colorado, *Transportation Research Record, No. 1290*, **1**(1991) 211-219.

4. Bruneau, M. and Zahrai, S. M., "Effect of corrosion on the ductility of steel members.", *Journal of Structural Engineering, ASCE*, No. 11, **123**(1997) 1478-1486.
5. American Society for Metal, "Atlas of fatigue curves", Edited by H.E. Boyer, Materials Park, Ohio, 1986.
6. Kulak, G. L., Fisher, J. W., and Struik, J. H. A., Guide to Design Criteria for Bolted and Riveted Joints. 2nd ed., John Wiley & Sons, New York, 1987.